Desalination and Water Treatment
www.deswater.com
doi: 10.1080/19443994.2015.1012749

57 (2016) 7047–7053
March

Taylor & Francis
Taylor & Francis Group

Easy simultaneous synthesis–immobilization of nanosized CuO–ZnO on perlite as a photocatalyst for degradation of acid orange 7 from aqueous solution in the presence of visible light

Ali Khani*, Bahar Pezeshki

Young Researchers and Elite Club, Miyaneh Branch, Islamic Azad University, Miyaneh, Iran, Tel. +98 41 52229377, Fax: +98 41 52227290; emails: a.khani59@yahoo.com, a.khani@m-iau.ac.ir (A. Khani), Tel. +98 9197443510; email: pezeshki.bahar@yahoo.com (B. Pezeshki)

Received 20 October 2014; Accepted 22 January 2015

ABSTRACT

In order to improve the photocatalytic activity, the researchers have loaded some metals or metal oxides on semiconductors such as TiO_2 and ZnO surface. This study investigated the degradation of acid orange 7 (AO7) from aqueous solution by prepared nanosized CuO–ZnO immobilized on expanded perlite (nCuO-ZnO-P) as a photocatalyst in the presence of visible light. First, nCuO-ZnO-P was simultaneously synthesized–immobilized by pyrolysis of previously adsorbed Cu^{2+} and Zn^{2+} on perlite at 723.15 K in oven. The results showed that, unlike ZnO, the prepared nanosized photocatalyst has an effective photocatalytic activity in the presence of visible light. The effective parameters on AO7 degradation which were evaluated in the designed batch photoreactor included initial concentration of AO7 (C_0), pH, the granule size of used perlite for immobilization (D), and temperature (T). It was found that the content of degradation was followed by increasing order: $C_0 = 15 > 25 > 35 > 45 > 55$ mg l^{-1}, pH $7 > 8 > 9 > 6 > 5$, $D = 0.50 > 0.75 > 1.00 > 1.25 > 1.50$ mm, and $T = 318.15 > 308.15 > 298.15 > 288.15 > 278.15$ K.

Keywords: Nanophotocatalyst; Synthesis–immobilization; Degradation; Visible light; Water treatment

1. Introduction

Textile, paper, and some other industries' wastewater contain residual dyes which are not readily biodegradable. Advanced oxidation processes (AOPs) are alternative techniques for removing dyes and many other organics in wastewater and effluents [1]. Semiconductor photocatalysts such as TiO_2 and ZnO are developed AOP, which can be conveniently applied to remove different organic pollutants [2]. In order to improve the photocatalytic activity, the researchers [3–9] focused their attentions on mixed oxide semiconductors due to the fact that an efficient charge separation can be obtained by coupling semiconductor particles with different energy levels [9–11]. Also, they were interested to increase the efficiency of photocatalytic reactions as a result of vectorial transfer of photogenerated electrons and holes from a semiconductor to another. There are a lot of reports about CuO–ZnO nanocomposites presently [12–14]; however, most of them are used for methanol synthesis, hydrogen production, gas sensor, and few are used for

*Corresponding author.

1944-3994/1944-3986 © 2015 Balaban Desalination Publications. All rights reserved.

photodegradation [9]. Synthesis of CuO–ZnO nanophotocatalyst for visible light-assisted degradation of a textile dye in aqueous solution has been reported by Sathishkumar et al. [9]. Saravanan et al. have studied enhanced photocatalytic activity of CuO–ZnO nanocomposite for the degradation of textile dye on visible light illumination [15]. Li and Wang have ferreted out synthesis and photocatalytic activity of CuO–ZnO nanocomposite for photodegradation of rhodamine B under the simulated sunlight irradiation [16].

In numerous investigations, an aqueous suspension of the catalyst particles has been used [17–19]. However, the use of suspensions requires separation and recycling of the ultrafine catalyst from the treated liquid and can be an inconvenient, time-consuming, and expensive process. The key to the problem of industrializing the technology seems to be simple and low-cost immobilization of catalysts [20–23] on solid media is suitable for the treatment process [24].

To circumvent the drawbacks, in the present study, the visible light was used instead of UV-C light because of its harmful and costly aspects and supported kind of photocatalyst was used instead of suspension photocatalyst. The reason for choosing copper oxide is due to its existence in stable form in atmospheric condition [25,26]. In addition, it is expected that the loaded CuO may improve photocatalytic activity of ZnO in the visible region, since the work function of CuO is quite similar to ZnO conduction band level and the standard reduction potential of oxygen molecule is considered to be probably an electron acceptor in ZnO aqueous suspension [9].

2. Experimental

2.1. Materials

The expanded perlite (perlite) used in the present study was obtained from Goohar Sahand Co. (Iran). Chemical composition and properties of the perlite are shown in Table 1. Acid orange 7 (AO7), as a target compound, was purchased from Boyakhsaz Co. (Iran). $Zn(NO_3)_2$ and $CuSO_4{\cdot}5H_2O$ were obtained from Merck (Germany). Deionized distilled water was used and all the experiments were repeated three times (variance (σ^2) = 0.008).

2.2. Preparation of nanosized CuO–ZnO immobilized on perlite (nCuO-ZnO-P)

The nanosized CuO–ZnO immobilized on perlite as a good support was prepared from pyrolysis of the previously adsorbed zinc nitrate and copper sulfate on perlite [1]. The solution of $Zn(NO_3)_2$ and $CuSO_4$ were stirred with perlite (the weight ratio of Cu:Zn:perlite was 1:3:10) in deionized distilled water for 30 min until zinc nitrate and copper sulfate adsorbed on expanded perlite, after which perlite was filtered and washed with the deionized distilled water and then heated to 723.15 K for 1 h in air oven for pyrolysis of zinc nitrate and copper sulfate to ZnO and CuO, respectively. To evaluate the supporting treatment, nZnO-CuO-P granules were leached twice with deionized distilled water and then dried. During treatment, the tangible weight difference was not observed which indicated good support. This method is easy, inexpensive, and effective, so exclusive for zinc oxide compared with TiO_2 as a standard semiconductor (because its salt is soluble in water that solubility is necessary in this method) [1]. By this method, synthesis and immobilization of nanosized CuO–ZnO on perlite was simultaneously performed.

Table 1
Chemical composition and properties of expanded perlite

Constituent	Percentage (Wt. %)
SiO_2, Al_2O_3, K_2O, CaO, Na_2O, Fe_2O_3, MgO, MnO_2	81, 11.4, 4.3, 0.9, 0.8, 0.7, 0.6, 0.2, 0.1
Properties	
Color	White
pH	7
Specific area	5.3 $m^2 g^{-1}$
Melting point	1573.15 K
Density	0.3 g cm^{-3}
Granule shape	Globular
Solubility in water	No soluble

2.3. Procedure

For the photodegradation of AO7, a solution containing the known concentrations of dye was prepared and then 1 L of the prepared solution was transferred into the designed photoreactor (Fig. 1), which consisted of jacketed cylindrical with conical bottom Pyrex (D = 5 cm and length = 20 cm) and agitated with a magnetic stirrer during the experiment. To explore the effect of pH, the solution's pH was initially adjusted at desired values by adding dilute NaOH and H_2SO_4 and by controlling with a pH meter (Philips PW 9422). The solution temperature was adjusted with a cooling system. Then the lamp (UV-C lamp: 8w-Philips and light intensity = 0.4 k Lux measured with a Lux-meter, Leybold-Heraeus and fluorescent (visible) lamp: 18w-Pars, Iran) was switched on to initiate the reaction. The concentration of the dye solution was determined with total organic carbon (TOC) analyzer (Shimadzu TOC-VCSH, North America). The degree of

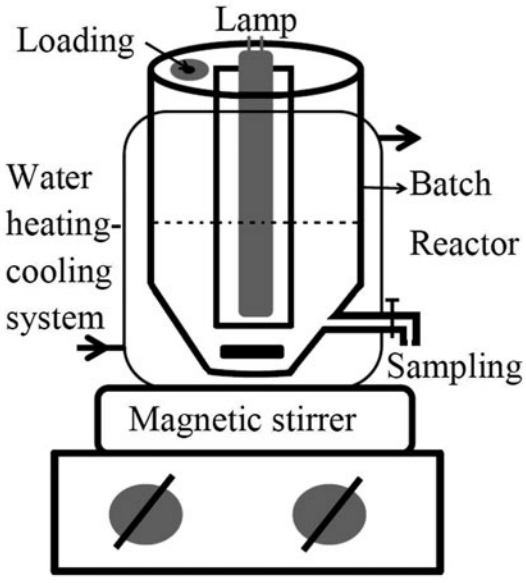

Fig. 1. The schematic diagram of experimental apparatus (photoreactor).

degradation of AO7 (removal efficiency) was calculated at different time intervals using the equation given below:

$$X\% = \frac{C_0 - C_t}{C_0} \times 100 \quad (1)$$

In which $X\%$ is the percentage of degradation, C_0 is the initial concentration of AO7, and C_t is the concentration of AO7 at time t.

2.4. XRD and SEM analysis methods

The average crystallite size (D in nm) of photocatalysts was determined using X-ray Diffraction (Bruker) pattern according to the Scherrer Eq. [1]:

$$D = k\left(\frac{\lambda}{\beta \cdot \cos\theta}\right) \quad (2)$$

where k is a constant which is 0.89, λ is the X-ray wavelength which is 0.154 nm, β is the full width at half maximum (0.0036 Radian), and θ is the half diffraction angle which is 18.

The morphology of the prepared catalysts and the perlite were determined using a Leo 440i scanning electron microscope (SEM) followed by AU coated by the sputtering method using a coater sputter SC 761.

3. Results and discussion

3.1. XRD and SEM analysis

The resulting graphs of the XRD analysis are shown in Fig. 2. This figure shows clearly the same pattern for the prepared nCuO-ZnO-P when compared to the standard CuO–ZnO powder. The result of the calculation shows that the average particle size is about 40 nm [1]. Fig. 3 shows the SEM image of the surface of the perlite and prepared photocatalyst. The images of perlite surface confirm the high porosity of perlite granules as a good support for the CuO–ZnO nanoparticles (Fig. 3(a)).

3.2. Control test

For the evaluation of the photocatalytic activity of the prepared photocatalyst, four experiments under basic conditions (initial concentration of AO7 = 35 mg l^{-1}, pH 7, the weight of nCuO-ZnO-P (perlite+ nCuO-ZnO) = 50 g, the granule size of perlite as a support = 4 mm, T = 298.15 K, the volume of solution = 1 L, and reaction time = 90 min) were designed in order to measure the degree of degradation in the presence of UV-C and/or Vis. lights (nCuO-ZnO-P/UV and or nCuO-ZnO-P/Vis.), the possibility of adsorption of AO7 on nCuO-ZnO-P in the darkness condition (nCuO-ZnO-P/darkness) and the possibility of photolysis of AO7 by UV-C light (UV-C only). TOC results showed (Fig. 4) that both the light (UV-C or visible) and the prepared photocatalyst were needed for the effective destruction of AO7. The degradation process has occurred in the

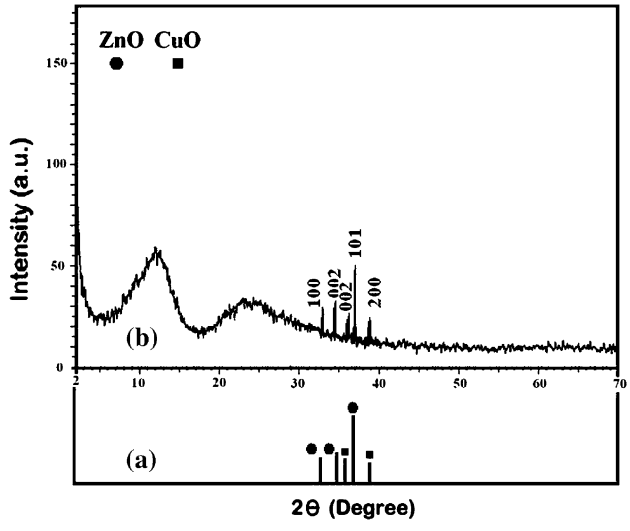

Fig. 2. Standard CuO–ZnO powder diffraction pattern (a) and XRD pattern of nanosized CuO–ZnO immobilized on perlite (b).

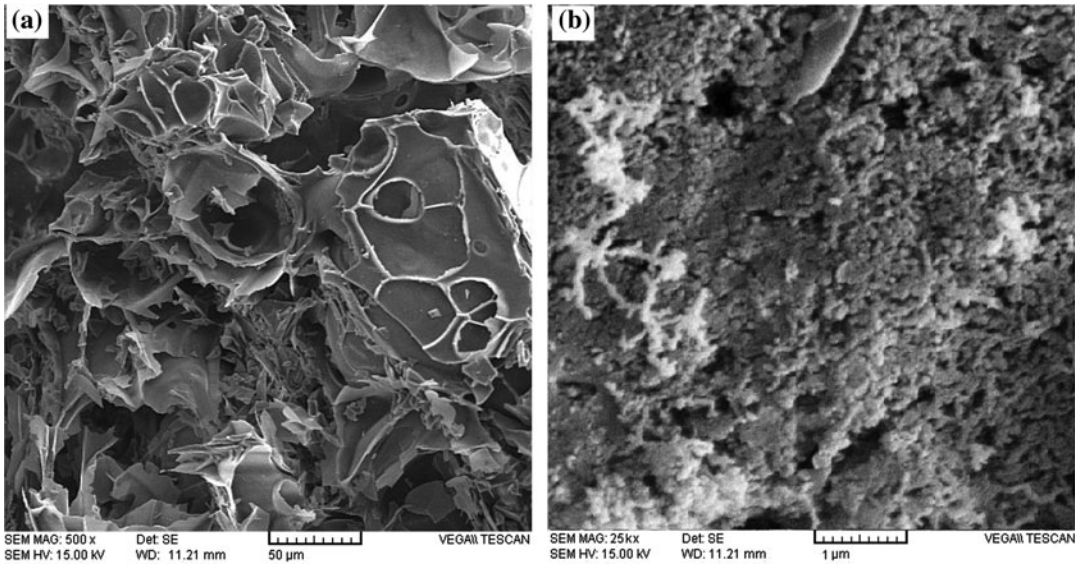

Fig. 3. SEM images of perlite (a) and nZnO-CuO-P (b).

presence of UV-C and visible light almost the same. In the presence of visible light, the percentage of mineralization was 90.82% under basic conditions. Also, Fig. 4 shows that nCuO-ZnO (in the darkness condition) and UV-C light do not affect the adsorption and or photolysis of AO7, respectively.

All of the following experiments were carried out in the presence of visible light.

3.3. Effect of initial dye concentration

For this purpose, the experiments were carried out with initial dye concentration, varying from 15 to 55 mg l^{-1} and other parameters were kept under basic conditions. The results show that degradation efficiency slightly decreases with an increase in the initial amount of AO7 (Table 2). The phenomenon may be attributed to two main factors. (1) At high dye concentration, the adsorbed dye molecules may occupy all the active sites of photocatalyst surface and this leads to decrease in degradation efficiency [27–29]. (2) Another reason may be due to the absorption of light photon by the dye itself leading to a lesser availability of photons for hydroxyl radical generation [1].

3.4. Effect of the initial pH

Electrokinetic studies have shown that the perlite samples have no iso-electric point and have negative zeta potential and surface charge [1]. The effect of pH on the photocatalytic degradation efficiency of AO7

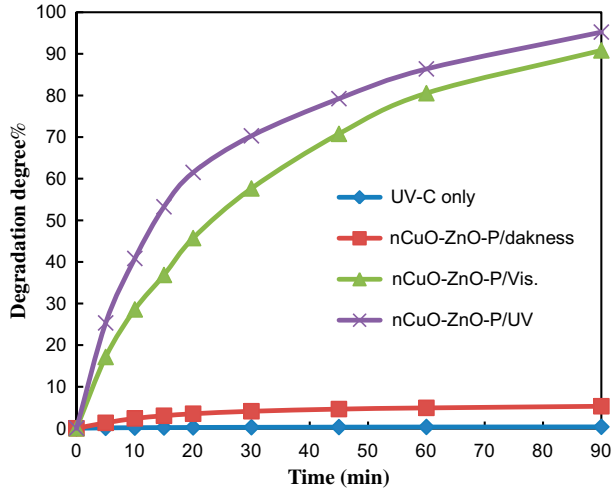

Fig. 4. Evaluation of the photocatalytic activity of the prepared photocatalyst in the presence of UV-C and Vis. lights (nCuO-ZnO-P/UV and nCuO-ZnO-P/Vis.), possibility of adsorption (nCuO-ZnO-P/darkness), and possibility of photolysis (UV-C only).

was examined at different pH ranging from 5 to 9 (Table 2). The results show that in alkaline solutions, photodegradation efficiency was more than that in acidic solutions. It is because photodecomposition of ZnO nanoparticles takes place in acidic and neutral solutions. The photocorrosion of ZnO nanoparticles is complete at pH lower than 6; and at higher pH, no photocorrosion of ZnO nanoparticles takes place. Since, AO7 has a sulfuric group in its structure, which

Table 2
The effect of some operational parameters on photodegradation process

Operational parameters	Degradation degree (X %)				
C_0 (mg l^{-1})	**15**	**25**	**35**	**45**	**55**
	98.51	96.23	90.82	85.23	81.95
pH	**5**	**6**	**7**	**8**	**9**
	53.89	60.28	90.82	77.77	65.84
D (mm)	**0.50**	**0.75**	**1.00**	**1.25**	**1.50**
	96.38	94.23	90.82	88.58	86.34
T (K)	**278.15**	**288.15**	**298.15**	**308.15**	**318.15**
	86.53	88.56	90.82	93.56	95.34

Note: The bold fonts indicate the value of operational parameters.

is negatively charged in alkaline conditions; therefore, in the alkaline solution, dye may not be adsorbed onto the photocatalyst surface effectively [1].

3.5. Effect of the granule size of used perlite for immobilization

First, different granule size of perlite (the specific area for granule size 0.50, 0.75, 1.00, 1.25, and 1.50 mm was 7.45, 7.16, 6.82, 6.51, and 5.85 $m^2 g^{-1}$, respectively) were used for synthesis–immobilization of nCuO-ZnO, then the effect of granule size of nCuO-ZnO-P on the degradation efficiency was studied. The results show that the degradation efficiency increases with a decrease in granule size of nCuO-ZnO-P (Table 2). This observation can be explained in terms of availability of active sites on the nCuO-ZnO-P surface. The total active surface area increases with decrease in granule size [1].

3.6. Effect of the temperature

To study the effect of temperature on degradation efficiency of nCuO-ZnO-P, the experiments were carried out with different temperatures varying from 278.15 to 318.15 K and other parameters were kept under basic conditions. The changes in dye concentration with time during the degradation process at each temperature show that the differences in the degradation efficiency of dye were small (Table 2). These small differences should originate from the effect of energy of reaction. For determination of activation energy (E_a) of reaction, at first, kinetics of the photocatalytic reactions was studied at different temperatures. In literature, photodegradation processes exhibited pseudo-first-order kinetics with respect to the concentration of the organic compound, by using the equation of given below [1].

$$r_R = \frac{-dC_R}{dt} = \frac{k_r K C_R}{1 + K C_R} \tag{3}$$

where r_R is the rate of reaction (degradation of the solute R), C_R is the solute concentration, t is the time of the reaction, and k_r and K are the reaction and adsorption constants associated with the solute, respectively. When the concentration is low, the term K_{CR} is often negligible, and the apparent reaction rate will follow a pseudo-first-order model. Integration of the equation under this assumption with boundary conditions of $C_R = C_{R0}$ at $t = 0$ yields:

$$-\ln\left(\frac{C_R}{C_{R0}}\right) = k_{app} t \tag{4}$$

where C_{R0} is the initial substrate concentration and k_{app} is the apparent first-orderreaction rate. The photocatalytic reactions in many cases show this behavior. Fig. 5 shows the plots of $-\ln(C_R/C_{R0})$ vs. t. The results show that reaction rate enhances as temperature increases from 278.15 to 318.15 K (Table 3).

A better criteria is to introduce a parameter known as normalized percent deviation, the lowest average absolute percent deviation (%D) or in some literature percent relative deviation modulus, P, given by the following Eqs. [1,2]:

$$P = \frac{100}{N} \sum \frac{|y_{exp} - y_{pred}|}{y_{exp}} \tag{5}$$

where y_{exp} is the experimental y at any x, y_{pred} is the corresponding predicted y according to the equation under study with best fitted parameters and N is the number of observations. It is clear that the lower the p value, the better is the fit. The fit accepted to be good when p is below 5 (Table 3).

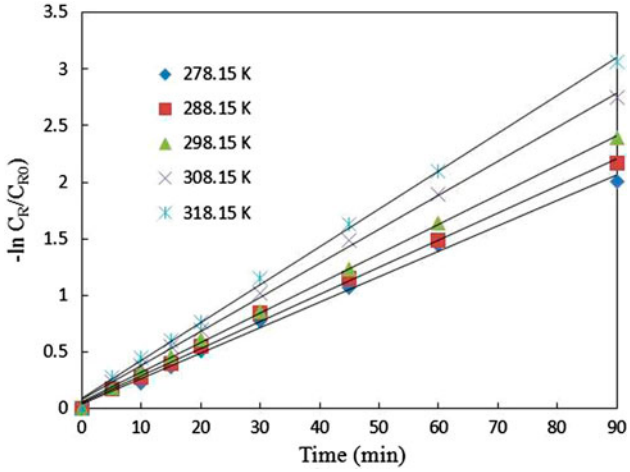

Fig. 5. The plots of $-\ln(C_R/C_{R0})$ vs. t.

Table 3
The rate constant of reaction in different temperatures

T (K)	278.15	288.15	298.15	308.15	318.15
R^2	0.996	0.997	0.999	0.998	0.998
P	0. 46	0.73	0.44	0.55	0.22
k_{app} (min^{-1})	0.022	0.024	0.026	0.030	0.033

For calculation of activated energy, the Arrhenius equation was used as [1]:

$$-\ln\ k = -\ln\ A + \frac{E_a}{R}\left(\frac{1}{T}\right) \quad (6)$$

where k = rate constant in min^{-1}, T = temperature in K.

The low activation energy (E_a) value (2.82 kJ mol^{-1}), calculated by Fig. 5 results (from the slope of line: −ln k vs. $1/T$), suggests that degradation of AO7 is limited by diffusion step and apparent rate constant reflects the rate at which AO7 molecules migrate from bulk solution to the reaction zone [1].

4. Conclusion

In this study nanosized CuO–ZnO immobilized on perlite was prepared via a simple and low-cost method. The results showed that the average particle size was about 40 nm. The photocatalytic degradation of AO7 which was confirmed with TOC analysis showed a good photocatalytic activity for the catalysts in visible light. Photolysis and adsorption were found to be negligible in overall degradation process. The degradation degree (X%) of photodegradation process was 90.82% under basic conditions. In the basis of P, pseudo-first- order kinetic model was confirmed for the reactions in the various temperatures. The activation energy of the reaction was 2.82 kJ mol^{-1}, suggesting a diffusion-controlled reaction.

Acknowledgments

The authors would like to thank the Young Researchers and Elite club, Miyaneh branch, Islamic Azad University for the financial support given for this study.

References

[1] A. Khani, M.R. Sohrabi, Simultaneous synthesis-immobilization of nano ZnO on perlite for photocatalytic degradation of an azo dye in semi batch packed bed photoreactor, Pol. J. Chem. Technol. 14 (2012) 69–76.
[2] A. Khani, M.R. Sohrabi, M. Khosravi, M. Davallo, Enhancing purification of an azo dye solution in nano-sized zero-valent iron-ZnO photocatalyst system using subsequent semi batch packed-bed reactor, Turk. J. Eng. Environ. Sci. 37 (2013) 91–99.
[3] Z.L. Liu, J.C. Deng, J.J. Deng, F.F. Li, Fabrication and photocatalysis of CuO/ZnO nano-composites via a new method, Mater. Sci. Eng., B 150 (2008) 99–104.
[4] N. Serpone, P. Maruthamuthu, P. Pichat, E. Pelizzetti, H. Hidaka, Exploiting the interparticle electron transfer process in the photocatalysed oxidation of phenol 2-chlorophenol and pentachlorophenol: Chemical evidence for electron and hole transfer between coupled semiconductors, J. Photochem. Photobiol., A: Chem. 85 (1995) 247–255.
[5] D. Chatterjee, Sh. Dasgupta, Visible light induced photocatalytic degradation of organic pollutants, J. Photochem. Photobiol. 6 (2005) 186–205.
[6] A. Di Paola, L. Palmisano, V. Augugliaro, Photocatalytic behavior of mixed WO_3/WS_2 powders, Catal. Today 58 (2000) 141–149.
[7] Y. Bessekhouad, D. Robert, J.V. Weber, Bi_2S_3/TiO_2 and CdS/TiO_2 heterojunctions as an available configuration for photocatalytic degradation of organic pollutant, J. Photochem. Photobiol., A: Chem. 163 (2004) 569–580.
[8] K.J. Green, R. Rudham, Photocatalytic oxidation of propan-2-ol by semiconductor-zeolite composites, J. Chem. Soc., Faraday Trans. 89 (1993) 1867–1870.
[9] P. Sathishkumar, R. Sweena, J.J. Wu, S. Anandan, Synthesis of CuO-ZnO nanophotocatalyst for visible light assisted degradation of a textile dye in aqueous solution, Chem. Eng. J. 171 (2011) 136–140.
[10] D. Zhang, Synthesis and characterization of ZnO-doped cupric oxides and evaluation of their photocatalytic performance under visible light, Transition Met. Chem. 35 (2010) 689–694.
[11] D. Zhang, F. Zeng, Structural, photochemical and photocatalytic properties of zirconium oxide doped TiO_2 nanocrystallites, Appl. Surf. Sci. 257 (2010) 867–871.
[12] D.F. Zheng, Preparation and photocatalytic properties of a kind of loaded photocatalyst of nanoscale CuO/ZnO composite, Pol. J. Chem. 83 (2009) 2009–2019.

[13] I. Eswaramoorthi, V. Sundaramurthy, A.K. Dalai, Partial oxidation of methanol for hydrogen production over carbon nanotubes supported Cu-Zn catalysts, Appl. Catal., A 313 (2006) 22–34.
[14] H.C. Yang, F.W. Chang, L.S. Roselin, Hydrogen production by partial oxidation of methanol over Au/CuO/ZnO catalysts, J. Mol. Catal. A 276 (2007) 184–190.
[15] R. Saravanan, S. Karthikeyan, V.K. Gupta, G. Sekaran, V. Narayanan, A. Stephen, Enhanced photocatalytic activity of ZnO/CuO nanocomposite for the degradation of textile dye on visible light illumination, Mater. Sci. Eng., C 33 (2013) 91–98.
[16] B. Li, Y. Wang, Facile synthesis and photocatalytic activity of ZnO-CuO nanocomposite, Superlattices Microstruct. 47 (2010) 615–623.
[17] S.R. Kanel, B. Manning, L. Charlet, H. Choi, Removal of arsenic (III) from groundwater by nanoscale zerovalent iron, Environ. Sci. Technol. 39 (2005) 1291–1298.
[18] S. Karri, R. Sierra-Alvarez, J.A. Field, Zero valent iron as an electron-donor for methanogenesis and sulfate reduction in anaerobic sludge, Biotechnol. Bioeng. 92 (2005) 810–819.
[19] B. Schrick, J.L. Blough, A.D. Jones, T.E. Mallouk, Hydrodechlorination of trichloroethylene to hydrocarbons using bimetallic nickel−iron nanoparticles, Chem. Mater. 14 (2002) 5140–5147.
[20] N.R.C.F. Machado, V.S. Santana, Influence of thermal treatment on the structure and photocatalytic activity of $TiO_2{\cdot}P_{25}$, Catal. Today 107 (2005) 595–601.
[21] W.J. Gong, H.W. Tao, G.L. Zi, X.Y. Yang, Y.L. Yan, B. Li, J.Q. Wang, Visible light photodegradation of dyes over mesoporous titania prepared by using chrome azurol S as template, Res. Chem. Intermed. 35 (2009) 751–762.
[22] Y. Cheng, H. Sun, W. Jin, N. Xu, Effect of preparation conditions on visible photocatalytic activity of titania synthesized by solution combustion Method, Chin. J. Chem. Eng. 15 (2007) 178–183.
[23] J. Medina-Valtierra, E.M. Moctezumab, C.J. Frausto-Reyes, Global photonic efficiency for phenol degradation and mineralization in heterogeneous photocatalysis, J. Photochem. Photobiol., A 174 (2005), 246–252.
[24] A. Khani, M.R. Sohrabi, M. Khosravi, M. Davallo, Decolorization of an azo dye from aqueous solution by nano zero-valent iron immobilized on perlite in semi batch packed bed reactor, Fresenius Environ. Bull. 21 (2012) 2153–2159.
[25] S. Eustis, D.C. Meier, M.R. Beversluis, B. Nikoobakht, Analysis of copper incorporation into zinc oxide nanowires, ACS Nano 2 (2008) 368–376.
[26] F.J. Sheini, J. Singh, O.N. Srivasatva, D.S. Joag, M.A. More, Electrochemical synthesis of Cu/ZnO nanocomposite films and their efficient field emission behaviour, Appl. Surf. Sci. 256 (2010) 2110–2114.
[27] A. Kesraoui-Abdessalem, N. Oturan, N. Bellakhal, M. Dachraoui, M.A. Oturan, Experimental design methodology applied to electro-Fenton treatment for degradation of herbicide chlortoluron, Appl. Catal., B 78 (2008) 334–341.
[28] W. Bahnemann, M. Muneer, M.M. Haque, Titanium dioxide-mediated photocatalysed degradation of few selected organic pollutants in aqueous suspensions, Catal. Today 124 (2007) 133–148.
[29] A.R. Khataee, M. Zarei, M. Fathinia, M. Khobnasab Jafari, Photocatalytic degradation of an anthraquinone dye on immobilized TiO_2 nanoparticles in a rectangular reactor: Destruction pathway and response surface approach, Desalination 268 (2011) 126–133.